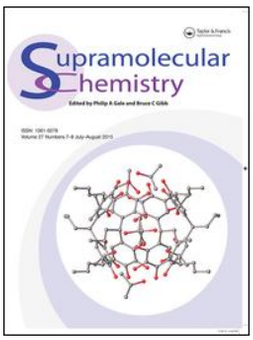

Supramolecular Chemistry

ISSN: 1061-0278 (Print) 1029-0478 (Online) Journal homepage: http://www.tandfonline.com/loi/gsch20

Synthesis, X-ray, ^{1}H-NMR and DFT analysis of the phthalimide–hydrazone probes as selective anion sensor

Priya Ranjan Sahoo, Kunal Prakash, Pragati Mishra, Palak Agarwal, Nikita Gupta & Satish Kumar

To cite this article: Priya Ranjan Sahoo, Kunal Prakash, Pragati Mishra, Palak Agarwal, Nikita Gupta & Satish Kumar (2016): Synthesis, X-ray, ^{1}H-NMR and DFT analysis of the phthalimide–hydrazone probes as selective anion sensor, Supramolecular Chemistry

To link to this article: http://dx.doi.org/10.1080/10610278.2016.1264074

SUPRAMOLECULAR CHEMISTRY, 2016
http://dx.doi.org/10.1080/10610278.2016.1264074

Taylor & Francis
Taylor & Francis Group

Synthesis, X-ray, ^{1}H-NMR and DFT analysis of the phthalimide–hydrazone probes as selective anion sensor

Priya Ranjan Sahoo, Kunal Prakash, Pragati Mishra, Palak Agarwal, Nikita Gupta and Satish Kumar

Department of Chemistry, St. Stephen's College, University Enclave, Delhi, India

ABSTRACT

Two simple phthalimide–hydrazone probes with nitro groups were synthesised and characterised by NMR, FT-IR, HR-MS and single crystal X-ray crystallography. The synthesised receptors were evaluated for application in anion sensing. The receptors displayed strong, sensitive and selective colouration in the presence of cyanide ions by forming a stable complex with cyanide ion. The use of variable nitro groups helped in the elucidation of the mechanism of the complex formation. The ^{1}H NMR spectroscopy was used to support the mechanism of the complex formation. DFT methods were used to understand the stability of the complex with respect to the reactant. The absorbance data were also compared with the TD-DFT calculated excitation parameters. The experimental results were found to correlate well with the theoretical data.

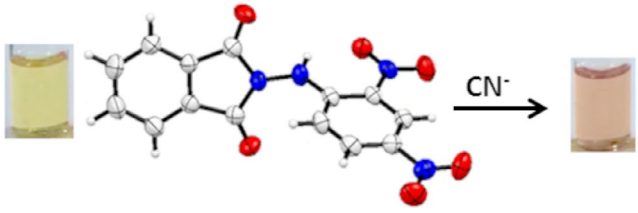

ARTICLE HISTORY
Received 16 September 2016
Accepted 20 November 2016

KEYWORDS
Phthalimide probe; hydrazone; cyanide ion; colorimetric detection; DFT

1. Introduction

Ubiquitous anions in small concentration play an essential role in many biological processes (*1, 2*). However, their presence beyond permissible limit is detrimental to environment and human health (*3, 4*). Therefore, serious environmental remediation efforts are required to identify and tackle the contaminated sites, which require a screening protocol consisting of library of potential receptors (*5*). Among the most abundant anionic pollutants, cyanide ion is known to have devastated effect on humans, plants as well as aquatic life (*6–9*). The widespread utilisation of cyanide in the production of organic chemical industry such as nylons and acrylics, etc. has further heightened the environmental concerns (*10*). The toxicity of cyanide ion is due to its tendency to irreversibly coordinate the trivalent iron present in the cytochrome c oxidase, which may result in a condition called hypoxia (*11, 12*). Synthetic receptors capable of binding selectively the analytes of interest is of huge significance (*13–16*). It is advantageous that the receptor shows sensitive, naked eye colorimetric response in the presence of suitable guest species for easy and affordable identification under practical conditions (*17, 18*). The general strategy for the detection of cyanide ion includes interaction with metal ion present in pyridine (*19*) or porphyrin core (*20*), quantum dots like CdSe (*21, 22*), boronic acid (*23, 24*), nucleophilic addition of cyanide ion to the photochromic molecules such as spiropyran (*25*) or naphthopyran (*26*) and the single electron transfer reactions (*27*). A number of reports related to cyanide detection with colorimetric response are available in the literature (*3, 11, 18, 28*). For example, a rhodfluor derivative displayed both colorimetric and fluorometric response in the presence of cyanide ions (*17*). The reported chemosensors for cyanide ions also include pyrrole-based receptors (*10*), subphthalocyanines (*29*) and functionalised calix[4] pyrrole (*30*).

In the recent past, there is a greater emphasis to develop small but competent molecules with H-bond motifs for anion sensing as strong anion binding is possible through H-bonding or electrostatic interactions (*31*). Hydrogen bonding is considered as one of the absolute

CONTACT Satish Kumar satish@ststephens.edu
Supplemental data for this article can be accessed http://doi.dx.org/10.1080/10610278.2016.1264074.

and prominent interaction in crystal stabilisation (*32–36*). At the same time, hydrogen bond is also essential for molecular interactions in the medicinal and biomedicinal field (*34, 37–39*). Recent research report highlights the use of phthalimide scaffolds in the areas of drug discovery and drug development (*40*). Such type of frameworks are potential agents as antimicrobial, antitubercular and antidiabetic markers (*41, 42*). The phthalimide derivatives and hydrazone functional moiety with hydrogen bond donor sites are also potential precursor for optical switches and sensors for environmentally relevant anions (*28, 43, 44*). It also help in tracing different anions in the agricultural habitat and hinterland (*45*). The multiple donor sites make these molecules more adaptable and adds significance as chelating agents (*46, 47*).

In the present article, we are reporting the synthesis, crystal structure, DFT and anion binding investigations of nitro group flanked phthalimide–hydrazone probes. The phthalimide–hydrazone probes can be used as a flexible and promising framework for real-time monitoring of toxic cyanide.

2. Experimental

2.1. Reagents

The reagents used in the study such as *o*-phthaloyl chloride, 2, 4-dinitrophenylhydrazine (99%), 4-nitrophenylhydrazine (98.5%), dichloromethane (99%, Anhydrous), dimethylsulfoxide(>99%), triethylamine (99%), tetrabutylammonium acetate (>98%), tetrabutylammonium hydrogen sulfate (99.5%), tetrabutylammonium bromide (99%), tetrabutylammonium dihydrogen phosphate (99%), tetrabutylammonium fluoride (>98%) and TRIS-Buffer (>99.9%) were purchased from Spectrochem, India. Tetrabutylammonium hexafluorophosphate (99%), and tetrabutylammonium nitrate (98+%) were purchased from Alfa Aesar. Tetrabutylammonium cyanide (>95%) was purchased from Sigma–Aldrich. Tetrabutylammonium iodide (99%) and tetrabutylammonium chloride (99%) were purchased from CDH India.

2.2. Instruments

The ^{1}H and ^{13}C NMR spectra were recorded on a 400 MHz Jeol ECX 400 NMR spectrometer. The NMR spectra were recorded either in DMSO-d_6 or $CDCl_3$. The chemical shift values of the signals are described in ppm relative to the TMS signal or residual solvent signal. In cases where solvent signal was used as reference, the solvent was assigned a value reported in the literature (*48*). The IR spectrum was recorded on a Perkin Elmer FT-IR-RXI spectrometer (with DTGS detector) using KBr pellet and 16 scans were performed. Single crystal data for receptor **1** and **2** was recorded on an Oxford Diffraction, X-calibur-S single crystal XRD machine.

2.3. UV–Vis studies

A solution of chelator **1** or **2** (1.0 mL, 5.0×10^{-5} M) was mixed with tetrabutylammonium salts of different anions (CN^-, F^-, OAc^-, Cl^-, Br^-, I^-, NO_3^-, $H_2PO_4^-$, HSO_4^-, PF_6^-, PhO^-, 1.0 mL, 5.0×10^{-5} M) in each experiment. The UV–visible spectra of the solutions were recorded on an Ocean Optics USB4000 UV–Visible spectrometer. Similarly, 2.0 mL solutions of **1** and **2** (1.96×10^{-5} M) with different anions (CN^-, F^-, OAc^-, Cl^-, Br^-, I^-, NO_3^-, $H_2PO_4^-$, HSO_4^-, PF_6^-, PhO^-, S^{2-}, SH^-, ClO_4^- = 1.96×10^{-5} M) in TRIS buffer (1.0 mM, pH 7.6) were prepared in a cuvette. The absorbance was recorded on an ocean Optics USB4000 UV–Visible spectrometer. For titration experiments, a solution of the receptor **1** or **2** (2.0 mL, 2.5×10^{-5} M) was taken in a quartz cuvette and titrated with a solution of tetrabutylammonium cyanide (1.0×10^{-3} M) in DMSO.

2.4. Computations

Calculations reported in this paper were performed using the Gaussian 09 rev. A.02 program suite (*49*). The initial geometry of the receptor **1** and **2** was generated using Gaussview 5.01 program. The geometries generated using Gaussview were optimised using DFT/B3LYP/6-31+G(d,p) and MPW1PW91/6-31+G(d,p) methods. The presence of local minimum state of the optimised structure was established through the absence of negative frequency. Polarisable continuum model (PCM) (*50*) was used to perform calculations in DMSO. The TD-DFT/B3LYP/6-31+G(d,p) and TD-DFT/MPW1PW91/6-31+G(d,p) were used to calculate the electronic excitation parameters for receptors **1**, **2** and their **1**-CN, **2**-CN complex.

2.5. Synthesis

2.5.1. Synthesis of receptor 1 (*51*)

To a solution of 4-nitrophenylhydrazine (1.0 g, 6.53 mmol) in a 100 mL round-bottom flask, dichloromethane (50 mL), triethylamine (0.5 mL) were added. The reaction mixture was stirred and *o*-phthaloyl chloride (0.36 mL, 2.78 mmol) was added dropwise to the reaction mixture in the round-bottom flask. The reaction mixture was allowed to stir for 3 h. The precipitate obtained was filtered and washed thoroughly with water. The product was recrystallised twice using hot methanol and dried. Yield 68%. m.p. 260–264 °C. FT-IR (KBr pellet, v/cm^{-1}): 3328, 2922, 1739, 1615, 1510, 1467, 1407, 1341, 1281 and 1234. ^{1}H NMR (400 MHz, $CDCl_3$, δ): 11.64 (*d*, 1H, NH), 8.06 (*d*, H,

Table 1. Experimental detail for receptors **1** and **2**.

Crystal data	**1**	**2**
Chemical formula	C14H9N3O4	C14H8N4O6
*M*r	283.24	328.2
Crystal system, space group	Orthorhombic, *P*212121	Orthorhombic, *Pna*21
Temperature (K)	297	293
a, *b*, *c* (Å)	5.2001 (10), 8.8939 (19), 26.026 (7)	5.3924 (2), 19.5141 (10), 13.0349 (7)
V (Å3)	1203.7 (5)	1371.64 (12)
Z	4	4
Radiation type	Mo *K*α	Mo *K*α
μ (mm^{-1})	0.12	0.13
Crystal size (mm)	0.03 × 0.02 × 0.02	0.02 × 0.01 × 0.01
Diffractometer	Xcalibur, Sapphire3	Xcalibur, Sapphire3
Absorption correction	Multi-scan *CrysAlis PRO*, Agilent-2013	Multi-scan *CrysAlis PRO*, Agilent-2013
T_{min}, T_{max}	0.219, 1.000	0.861, 1.000
No. of measured, independent and observed [$I > 2\sigma(I)$] reflections	9273, 2247, 1683	17,658, 3467, 2661
*R*int	0.074	0.055
(sin θ/λ)max (Å−1)	0.605	0.691
R[*F*2 > 2σ(*F*2)], *wR*(*F*2), *S*	0.068, 0.130, 1.09	0.044, 0.097, 1.06
No. of reflections	2247	3467
No. of parameters	190	218
No. of restraints	0	1
H-atom treatment	H-atom parameters constrained	H-atom parameters constrained
$\Delta\rho_{max}$, $\Delta\rho_{min}$ (e Å−3)	0.20, −0.18	0.15, −0.14
Absolute structure	Flack x determined using 425 quotients [(*I*+)−(*I*−)]/[(*I*+)+(*I*−)] (*52*)	Flack x determined using 969 quotients [(*I*+)−(*I*−)]/[(*I*+)+(*I*−)] (*52*)
Absolute structure parameter	2.8 (10)	0.0 (8)

J = 9.2 Hz, ArH), 7.90–7.88 (*m*, 2H, ArH), 7.80–7.78 (*m*, 2H, ArH), 6.77 (*d*, 2H, *J* = 9.2 Hz, ArH). ^{13}C NMR (100 MHz, DMSO-d_6): 167.6, 154.8, 137.9, 134.6, 130.3, 128.1, 125.6, 110.9. HR-MS: m/z = Calculated [M + H] 284.0671 found [M + H] = 284.0662.

2.5.2. Synthesis of receptor 2

To a solution of 24-dinitrophenylhydrazine (1.0 g, 5.04 mmol) in a 100 mL round-bottom flask, dichloromethane (50 mL), triethylamine (0.5 mL) were added. The reaction mixture was stirred and *o*-phthaloyl chloride (0.30 mL, 2.32 mmol) was added dropwise to the reaction mixture in the round-bottom flask. The reaction mixture was allowed to stir for 3 h. The precipitate obtained was filtered and washed thoroughly with water. The product was then recrystallised from hot methanol and dried. Yield 72%. m.p. 240–245 °C. FT-IR (KBr pellet, v/cm^{-1}): 3266, 2918, 1779, 1583, 1535, 1471, 1311 and 1257. ^{1}H NMR (400 MHz, DMSO-d_6): δ = 11.27 (*s*, 1H, NH), 8.17 (*d*, 2H, *J* = 9.2 Hz, ArH), 8.01 (*d*, 1H, *J* = 8.4 Hz, ArH), 7.93 (*t*, 1H, *J* = 7.6 Hz, ArH), 7.75 (*t*, 1H, *J* = 7.6 Hz, ArH), 7.43 (*d*, 2H, *J* = 9.2 Hz, ArH). ^{13}C NMR (100 MHz, $CDCl_3$, δ): 168.0, 155.2, 145.1, 137.6, 131.8, 131.1, 129.9, 128.8, 123.5, 116.3. HR-MS: (*m/z*) = Calculated [M + H] 329.0522 found [M + H] = 329.0506.

2.6. Crystal data

The detailed crystal data, collection and structure refinement parameters for **1** and **2** are summarised in Table 1 (*52*). Olex2 (*53*) GUI was employed to solve the structure using the ShelXT/direct method (*54*) structure solution program and refined using ShelXL/least square (*55*) program. All the non-hydrogen atoms in the receptor **1** and **2** were refined anisotropically. All the aromatic H atoms were placed at their calculated position (C–H = 0.93 Å) and treated using a riding model with $U_{iso}(H) = 1.2U_{eq}(C)$. The N–H atoms in both **1** and **2** were located, fixed at N–H = 0.86 Å and refined freely. Mercury software (*56*) was used to prepare the graphics material for publication.

The crystallographic data for both the receptors (**1** and **2**) were deposited to the CCDC, 12 Union Road, Cambridge CB2 1EZ, UK. The copies of the data can be obtained free of charge on request, by quoting the deposition numbers 1432915, 1420924 and the publication citation.

3. Results and discussion

The phthalimide–hydrazone probes were synthesised as per the Scheme 1 in 68–72% yield. The receptors were characterised using IR, NMR, HRMS and single crystal X-ray crystallography.

3.1. X-ray crystallography

The crystals of receptors **1** and **2**, suitable for single crystal X-ray crystallographic determination were grown through slow evaporation of a methanolic solution. X-ray diffraction analysis revealed that the receptor **1** crystallised in $P2_12_12_1$ space group, while receptor **2** crystallised in $Pna2_1$ space group (Figure 1). The two aromatic units of both the

receptor **1** and **2** were observed to be almost orthogonal to each other. In receptor **1**, the two aromatic units displayed torsion angles of 98.35(3)° [C_{17}-C_{18}-C_{10}-C_{16}] and 49° [C_{21}-C_{11}-C_{10}-C_{16}] with respect to each other, while in receptor **2**, the two aromatic units displayed torsion angles of 100.2(1)° [C_{21}-C_{22}-C_{20}-C_{11}] and 47.3(6)° [C_{24}-C_{18}-C_{12}-C_{17}] with respect to each other. Both the receptor **1** and **2** displayed similar N–N–C angles. The N_4-N_3-C_{10} angle was observed to be 119.8(4)° in receptor **1**, while N_5-N_9-C_{12} angle was observed to be 120.57(3)° in receptor **2**. A N–N–C angle around ~120° in both the receptors (**1** and **2**) may allow the N–H group to easily participate in intermolecular H-bond formation or interact with an ionic species (Tables 2 and 3, Figure S1, Figure S2 ESI). The crystal packing revealed the formation of intermolecular hydrogen bond in both **1** and **2** (Table 2, Figures S1 and S2). The intermolecular hydrogen bonding was observed between N_3–H_3···O_1^{i} ((i) $-x, y + 1/2, -z-3/2$) and N_3–H_3···O_2^{ii} ((ii) $x + 1, y, z$) in receptor **1** (Table 2), while receptor **2** displayed intermolecular H-bond between O_{01}····H_{09}–N_{09} (Table 3). The parameters for N_3–H_3···O_1^{i} ((i) $-x, y + 1/2, -z-3/2$) and N_3–H_3···O_2^{ii} ((ii) $x + 1, y, z$) indicate that the former is stronger than the latter. Unlike receptor **1**, the crystal structure or receptor **2** displayed the intramolecular H-bonding (Table 3). The crystal packing also revealed the presence of several weak C–H···O and C–H···N interactions, which link the molecules together into three-dimensional network (Tables 2 and 3, Figures S1 and S2).

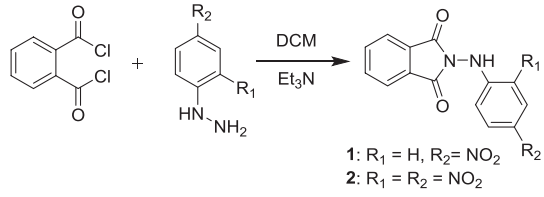

Scheme 1. The synthesis route of the receptor **1** and **2**.

3.2. Naked eye detection

The synthesised receptors were evaluated through colorimetric response for affinity towards different environmentally and biologically important anions due to the presence of the acidic N–H group available for intermolecular H-bond formation in DMSO and DMSO:water (8:2, 1.0 mM TRIS buffer, pH 7.6). Standard solutions of the receptors **1** and **2** (1.0×10^{-4} M) were prepared in DMSO and treated with one equivalent tetrabutylammonium salts of different anions (CN^-, F^-, OAc^-, Cl^-, Br^-, I^-, NO_3^-, $H_2PO_4^-$, HSO_4^-, PF_6^-, S^{2-}, SH^-, ClO_4^-, PhO^-) in DMSO. The colorimetric investigation revealed that the receptor **1** and **2** can detect the presence of cyanide ion selectively by displaying a colour change visible to the naked eye (Figures 2 and 3). The addition of tetrabutylammonium salt of cyanide ion to a solution of **1** in DMSO produced the colour change of the solution from colourless to dark yellow, while the addition of cyanide ions to receptor **2** in DMSO produced a colour change from yellow to orange-red (Figure 3). The colour change observed for receptor **1** in the presence of cyanide

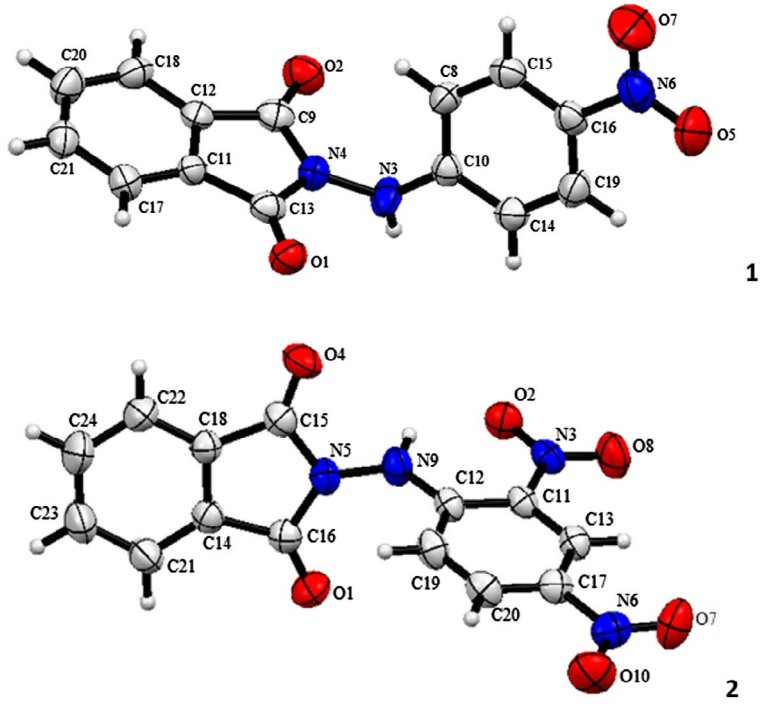

Figure 1. (Colour online) ORTEP view of crystal structure of the receptors **1** and **2** with displacement ellipsoids at the 50% probability level.

changes to light yellow with time. However, unlike receptor **1**, the colour change for receptor **2** was immediate and no colour change with time was observed. No colour change was observed in the solution of receptor **1** and **2** upon addition of other anions (Figures 2 and 3). When the similar experiments were repeated to evaluate the affinity of receptor **1** and **2** towards anions in DMSO:water (8:2, 1.0 mM TRIS buffer, pH 7.6), an immediate colour change from colourless to light purple was observed for receptor **1** (Figure S3). The receptor **2** produced a colour change from light yellow to dark yellowish-red in the presence of cyanide ion (Figure S4). The colour change for both receptors **1** and **2** remained unchanged with time. However, no colour change was observed upon addition of other anions (F^-, OAc^-, Cl^-, Br^-, I^-, NO_3^-, $H_2PO_4^-$, HSO_4^-, PF_6^-, S^{2-}, SH^-, ClO_4^-, PhO^-). The observation indicated that the receptors **1** and **2** act as selective sensor of cyanide ions.

The observations also suggested that due to the presence of two electronegative groups in receptor **2** the N–H proton is highly acidic and was easily abstracted by the cyanide ions. The presence of two nitro groups intensified the observed colour change. The nitro groups are known to influence the charge separation in the receptors (*57*) and help in the anion coordination (*58*). Anion coordination is also attributed to hydrogen bond interactions (*59*) with the binding sites consisting of a highly polarised N–H group (*16, 60*). The anions may deprotonate highly polarised N–H groups, which produce considerable electron delocalisation resulting in the colour change visible to naked eye and shift in absorption band (*61*). In addition, the fact that both receptors **1** and **2** selectively complex a less basic cyanide ion in comparison to other anions indicate (pKa: F^- = 15, CN^- = 12.9, OAc^- = 12.6, Cl^- = 1.8, Br^- = 0.9) (*62*) that the recognition event is dictated by factors such as pKa, size, geometry and nucleophilicity of the anion. Although similar change in colour was observed in a tweezer-shaped receptor composed of two 24-dinitrophenylhydrazone

Table 2. Short intermolecular contacts observed in receptor **1**.

D–H···*A*	*D*–H (Å)	H···*A* (Å)	*D*···*A* (Å)	*D*–H···*A* (°)
N_3–H_3···O_1^{i}	0.848(5)	2.590(5)	3.288(5)	140.46(44)
N_3–H_3···O_2^{ii}	0.848(5)	2.641(5)	3.365(6)	144.21(45)
C_8–H_8···O_1^{iii}	0.930(5)	2.648(3)	3.573(6)	172.4(31)
C_8–H_8···N_4	0.930(5)	2.602(4)	2.854(6)	96.10(31)
C_{14}–H_{14}···O_1^{i}	0.930(5)	2.837(3)	3.603(6)	140.38(31)
C_{15}–H_{15}···O_7	0.930(5)	2.403(5)	2.702(7)	98.49(34)
C_{19}–H_{19}···O_5^{iv}	0.930(5)	2.807(4)	3.729(7)	171.18(35)
C_{19}–H_{19}···O_5	0.930(5)	2.448(5)	2.730(7)	97.50(34)

Symmetry codes: (i) $-x, y + 1/2, -z-3/2$; (ii) $x + 1, y, z$; (iii) $x-1, y, z$; (iv) $x + 1/2, -y-1/2, -z-1$.

Table 3. Short intermolecular and intramolecular contacts observed in receptor **2**.

D–H···*A*	*D*–H (Å)	H···*A* (Å)	*D*···*A* (Å)	*D*–H···*A* (°)
N_{09}–H_{09}···O_{01}^{i}	0.924(3)	2.529(2)	3.048(2)	115.90(5)
N_{09}–H_{09}···O_{02}	0.924(3)	1.916(3)	2.588(3)	127.89(3)
N_{09}–H_{09}···N_{03}	0.924(3)	2.905(4)	2.905(3)	102.12(2)
C_{13}–H_{13}···O_{07}	0.931(3)	2.411(3)	2.711(4)	98.57(2)
C_{13}–H_{13}···O_{08}	0.931(3)	2.338(3)	2.659(3)	99.79(2)
C_{19}–H_{19}···O_{04}^{ii}	0.930(3)	2.607(3)	3.362(4)	138.70(2)
C_{19}–H_{19}···N_{05}	0.930(3)	2.478(3)	2.793(4)	99.94(2)
C_{19}–H_{19}···O_{07}^{iii}	0.930(3)	2.789(3)	3.470(4)	130.90(2)
C_{20}–H_{20}···O_{10}	0.930(3)	2.457(3)	2.730(4)	96.95(2)
C_{23}–H_{23}···O_{07}^{iv}	0.930(4)	2.808(3)	3.218(5)	107.90(2)
C_{24}–H_{24}···O_{07}^{v}	0.930(4)	2.879(3)	3.571(5)	132.23(2)
C_{24}–H_{24}···O_{08}^{iv}	0.930(4)	2.952(3)	3.636(5)	131.58(2)

Symmetry codes: (i) $x-1/2, -y + 1/2, z$; (ii) $x + 1, y, z$; (iii) $-x + 2, -y + 1, z + 1/2$; (iv) $x, y, z + 1$; (v) $x-1, y, z + 1$.

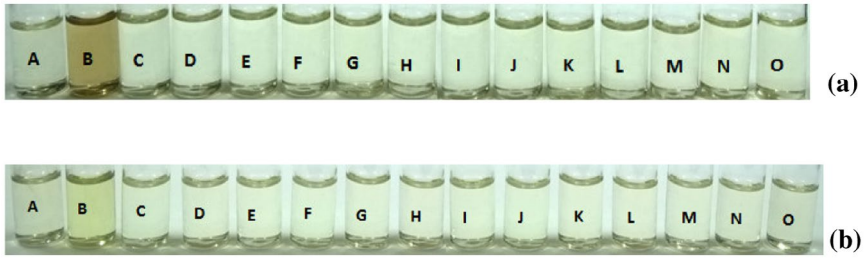

Figure 2. (Colour online) Colour change on addition of 1.0 equivalent of tetrabutylammonium salt of anions into a solution of phthalimide receptor **1** in DMSO (a) immediate change in colour, (b) Colour of the solution after 1 min.
Notes: [**1**] = 2.5×10^{-5} M. From left to right; A = Free receptor, B = CN^-, C = F^-, D = OAc^-, E = Cl^-, F = Br^-, G = I^-, H = NO_3^-, I = $H_2PO_4^-$, J = HSO_4^-, K = PF_6^-, L = PhO^-, M = ClO_4^-, N = S^{2-}, O = SH^-.

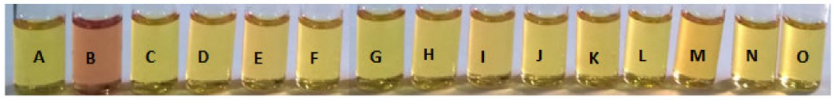

Figure 3. (Colour online) Colour change on addition of 1.0 equivalent of tetrabutylammonium anions into a solution of hydrazone receptor **2** in DMSO.
Notes: [**2**] = 2.5×10^{-5} M. From left to right; A = Free receptor, B = CN^-, C = F^-, D = OAc^-, E = Cl^-, F = Br^-, G = I^-, H = NO_3^-, I = $H_2PO_4^-$, J = HSO_4^-, K = PF_6^-, L = PhO^-, M = ClO_4^-, N = S^{2-}, O = SH^-.

moieties, but the mechanism of complex formation differ slightly (*16*). The complex formation in the tweezer-shaped molecule with two 24-dinitrophenylhydrazone groups involved additional step, which require displacement of DMSO by cyanide ion. This vital step required for the formation of complex was absent in the case of receptors **1** and **2**. The design for the phthalimide–hydrazone probe (**1** and **2**) is simple and comparable in efficiency to the tweezer-shaped molecule reported in the literature (*16*).

3.3. UV–visible studies

The process of complex formation between receptors (**1** and **2**) and cyanide ion was further explored using UV–Visible spectroscopy. The UV–visible spectra of receptor **1** displayed an absorption band between 350 and 470 nm. The addition of one equivalent cyanide ions into a solution of receptor **1**, leads to the decrease in the receptor **1** absorption band at 420 nm and appearance of a new band at 600 nm (Figure 4). The absorption band at 600 nm disappeared with time with the appearance of a new band at 480 nm (Figure S5). No other anions produced any change in the absorbance spectra of the receptor **1** (Figure 3). In order to understand the observed spectral shift from 600 to 480 nm in DMSO for **1**, a solution of receptor **1** was treated with one equivalent of cyanide ion and the spectra were recorded with time (Figure S5). The rate of disappearance of band at 600 nm was plotted against time, an exponential decay was observed (Figure S6). The shift in absorption maxima from 600 to 480 nm followed first-order reaction kinetics. The data obtained were applied to first-order reaction kinetics and the rate constant for this reaction was calculated (Figure S7). The appearance of a band at 600 nm indicated a complex formation between the cyanide ion and the receptor **1** through the H-bond between N–H and CN^- ion. The complex formation further resulted in the abstraction of a proton by the cyanide ion, which yielded the anion of the receptor **1** and HCN as products. The process is slow enough to allow kinetic measurement through UV–visible spectroscopy. The proton abstraction by anions in receptors with acidic hydrogen was reported earlier in the literature (*63*), which results in the formation of a coloured species.

A similar absorbance band at ~485 nm was observed, when a solution of the receptor **1** was treated with cyanide ions under pH controlled conditions in DMSO: water (8:2, 1.0 mM Tris buffer, pH = 7.6) solvent system. The absence of any change in the absorption spectra of the receptor **1** in the presence of other anions indicated the selectivity of the receptor **1** towards cyanide ion (Figure S8). No change in absorbance with time was observed under pH controlled conditions. The receptors (**1** and **2**) displayed a bathochromic shift in the UV–visible, while the receptors that recognise the cyanide ions through covalent linkage with cyanide ion display a hypsochromic shift with respect to their open coloured form (merocyanine form) (*25, 26*). The colour change here is more intense in comparison to the naphthopyran receptor (*26*) or spiropyran-based receptors (*25*).

Similarly, the solution of receptor **2** in the presence of one equivalent anions (tetrabutylammonium salt) was analysed through UV–visible spectroscopy, a decrease in intensity of the absorption band at 340 nm was observed, while a band at 410 nm with shoulder at 480 nm increased in intensity (Figure 5). No colour change was observed in the presence of tetrabutylammonium salt of other anions

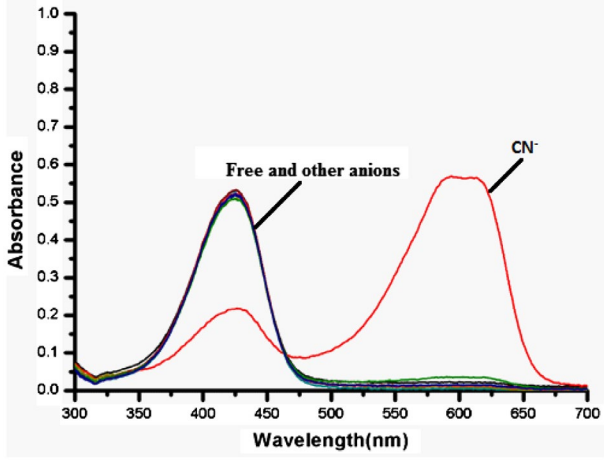

Figure 4. (Colour online) Absorption spectra of receptor **1** ([**1**] = 2.5×10^{-5} M) with 1.0 equivalent of tetrabutylammonium salt of various anions (CN^-, F^-, OAc^-, Cl^-, Br^-, I^-, NO_3^-, $H_2PO_4^-$, HSO_4^-, PF_6^-, S^{2-}, SH^-, ClO_4^-, 2.5×10^{-5} M) or NaOPh in DMSO.
Note: For simplicity spectra of only few important anions are shown.

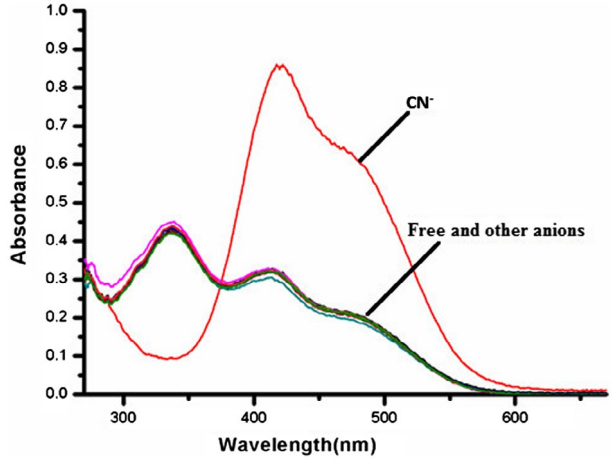

Figure 5. (Colour online) Absorption spectra of **2**([**2**] = 2.5×10^{-5} M) with 1.0 equivalent amounts of tetra-*n*-butyl ammonium salt of various anions (CN^-, F^-, OAc^-, Cl^-, Br^-, I^-, NO_3^-, $H_2PO_4^-$, HSO_4^-, PF_6^-, PhO^-Na^+, S^{2-}, SH^-, ClO_4^-, 2.5×10^{-5} M) in DMSO.
Note: For simplicity spectra of only few important anions are shown.

(F^-, OAc^-, Cl^-, Br^-, I^-, NO_3^-, $H_2PO_4^-$, HSO_4^-, PF_6^-, PhO^-, S^{2-}, SH^-, ClO_4^-). Under pH controlled conditions, a spectral shift from 370 nm to 440 nm was observed in the absorption spectra of receptor **2** upon addition of one equivalent cyanide ion in DMSO:water (8:2, 1.0 mM TRIS, pH 7.6) (Figure S9). No spectral shift in the absorption spectra was detected in the presence of other anions (F^-, OAc^-, Cl^-, Br^-, I^-, NO_3^-, $H_2PO_4^-$, HSO_4^-, PF_6^-, S^{2-}, SH^-, ClO_4^-, PhO^-). The results indicate that the receptor **2** can be used for selective detection of cyanide ions.

To further evaluate the strength of complex between the receptors (**1** and **2)** and cyanide ion, UV-Visible titration experiments were performed in DMSO. Upon gradual addition of cyanide ion to the receptor **1** solution, the peak at 420 nm gradually reduced followed by the development of a new peak at 600 nm, which gradually reduced in intensity with time and a new band appeared at 480 nm (Figure S10). Similarly, a solution of receptor **2** was titrated with a solution of cyanide ions in DMSO. The gradual addition of cyanide ions into a solution of receptor **2** in DMSO results in the increase in absorption intensity of a band at 410 nm and a clearly distinguishable isosbestic point at 370 nm, which indicated the formation of a stable complex between the receptor **2** and cyanide ion (Figure S11).

The experimental titration data were analysed using the HypSpec program (*64*) to obtain the value of association constant through nonlinear fit. Different binding equilibria (Scheme 2) were considered between the receptors (**1** and **2)** and cyanide ions. The experimental data were either applied to single equilibria model 1:1 (A:B) using only equation 1 or any of the multiple binding equilibria models such as 1:1 (A:B)+1:2 (A:2B) model using equation 1 and 2, 1:1 (A:B)+2:1 (2A:B) model using equation 1 and 3 and (A:B)+1:2 (A:2B)+2:1 (2A:B) model using equation 12 and 3 to observe better data fit with HypSpec program. The single equilibria model 1:1 (AB) considers that one molecule of receptor binds to one molecule of the anion (equation 1). The result of the analysis using HypSpec provides association constant K_{11}. The data can also be applied to multiple equilibria model 1:1 (A:B)+2:1 (2A:B), which consider equation 1 and 2, the result of the analysis using HypSpec can provide both K_{11} and K_{21}. Another multiple binding model 1:1 (A:B)+1:2 (A:2B) consider equation 1 and 3 for the calculations and the result of the analysis using HypSpec can provide both K_{11} and K_{12}. The

$$A + B \underset{}{\overset{K_{11}}{\rightleftharpoons}} C \quad \text{------ Equation 1}$$

$$C + A \underset{}{\overset{K_{21}}{\rightleftharpoons}} D \quad \text{------ Equation 2}$$

$$C + B \underset{K_{12}}{\rightleftharpoons} E \quad \text{------ Equation 3}$$

Scheme 2. Binding models used to fit the experimental data.

experimental data for both the receptors (**1** and **2**) were tested against all the different type of binding equilibria models shown in Scheme 2. The 1:1 binding model, which utilises only equation 1 was observed to fit better with the experimental data for both the receptors and provided a logβ value of 4.379 ± 0.005 (Figure S12) for receptor **1** and 4.8776 ± 0.0475 (Figure S13) for receptor **2**. The other binding equilibria models, which consider equation 1 with equation 2 or 3 or both did not provide a good fit between the experimental and observed absorbance values. A high logβ value of the association constant support the observation that the receptors **1** and **2** have a high affinity for cyanide ion and receptor **2** forms a slightly stronger complex with cyanide ion in comparison to the receptor **1**. The 1:1 complex stoichiometry was further supported by Job's plot (Figures S14 and S15).

3.4. NMR studies

The ^{1}H NMR spectra were used to further investigate the interaction between the receptors and cyanide ions. The ^{1}H NMR of receptor **2** and **2**-CN complex indicates that the –NH signal at δ11.27 ppm disappeared upon addition of cyanide ions, while a new peak at δ8.27 ppm appeared. A new signal at δ8.14 ppm was also seen in the ^{1}H NMR spectra of receptor **1** with cyanide ions (Figures 6 and S18). The appearance of new signal may be attributed to the formation of HCN complexed to the nitrogen atom of the receptor molecule. The observation supports the deprotonation mechanism for the complex formation between the receptors and the cyanide ion. The shielding of all ^{1}H NMR signals further supports the deprotonation in the presence of cyanide ions (Figure 6).

3.5. Practical utility

To investigate the practical utility of the receptors **1** and **2**, the detection limit of the both receptors (**1** and **2**) towards

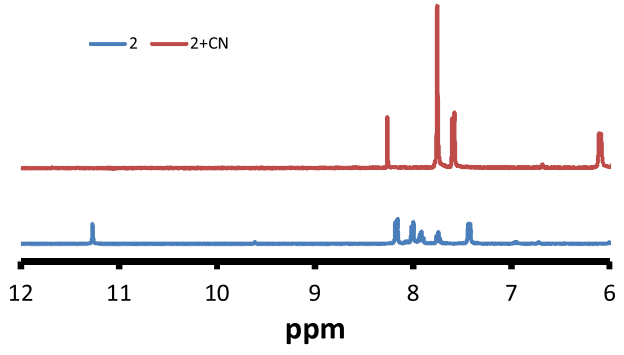

Figure 6. (Colour online) Partial ^{1}H NMR spectra of **2** and **2**-CN complex recorded in DMSO-d_6.

cyanide ion was determined using the method reported in the literature (*65*). A plot was drawn between absorbance and [CN^-], which produced a linear change in absorbance intensity on increasing cyanide ion concentration (Figures S16 and S17). The slope (*m*) and the standard deviation (σ) were used for the calculation of detection limit based on $3\sigma/m$. A detection limit value of 5.18 μM for receptor **1** and 0.48 μM for receptor **2** was obtained using the experimental data. The detection limit value observed for receptor **1** is above the detection limit value (1.9 μM) recommended by WHO (*8*) but lower than the EPA recommended limit of cyanide concentration (7.8 μM) (*66, 67*) in drinking water. The detection limit value obtained obtained for receptor **2** is lower than the concentration limit recommended by WHO (1.9 μM) (*8*) and EPA (7.8 μM) (*66, 67*) in drinking water**.** The detection limit value obtained for the receptor **2** was comparable to the detection limit of the optical (both colorimetric and fluorometric) sensors (*19, 24, 68–73*) reported in the literature. It should also be noted that the receptors reported in the literature often required light to induce cyanide binding, while the receptors **1** and **2** displayed colour change without any requirement of light or dark conditions (*24–26, 68–71*). Some receptors reported for the detection of cyanide ions are employed in the pure organic solvents, while the receptors **1** and **2** detected cyanide ions in both organic and aqueous organic solvents (*26, 74*) with a comparable detection limit. The limit of detection value indicated that the receptor **2** is more sensitive and simple colorimetric sensor for cyanide ion in comparison to the similar tweezer-shaped receptor reported in the literature (*16*).

To explore the practical applications of the synthesised receptor, paper strips of receptors (**1** & **2**) were prepared by dipping the filter paper strips in a solution of the receptors (1.0×10^{-5} M). The paper strips were dried in the air, followed by treatment with a solution of cyanide ions (1.0×10^{-5} M) in aqueous DMSO. A clear change in colour visible to the naked eye was observed, which indicated that both the receptors can be used for the detection of cyanide ions (Figures 7 and 8).

3.6. Computational studies

To understand further the process of complex formation between the receptors and the cyanide ions, DFT calculations were performed using the Gaussian 09 software suite. DFT/B3LYP methods are successfully used to study a number of processes, which include photochromism, enzymatic process, catalysis employing zeolites, drug design, solar energy and supramolecular chemistry (*75–79*). However, in certain systems, DFT methods fail to predict the ground state correctly (*80*). DFT methods badly describe the dispersion interactions and are not used to study the stacking or London-type interactions (*81–83*). However, such failures are rare and DFT methods provide excellent results for certain supramolecular systems (*84, 85*). The results of the study were compared with new hybrid density functional model MPW1PW91. The MPW1PW91 method is known to provide accurate results for non-covalent interactions (*86, 87*). The structure of the receptor **1**, **2** and their complex with cyanide ion were optimised using DFT/B3LYP/6-31+G(d,p) method. The energies of the optimised geometries (Figure 9) are listed in the Table 4.

The important geometrical parameters obtained through the computational methods were compared with the parameter obtained using X-ray crystallography data. A good correlation between the geometrical parameters (bond angles and bond lengths) calculated using DFT methods and obtained through X-ray crystallographic data

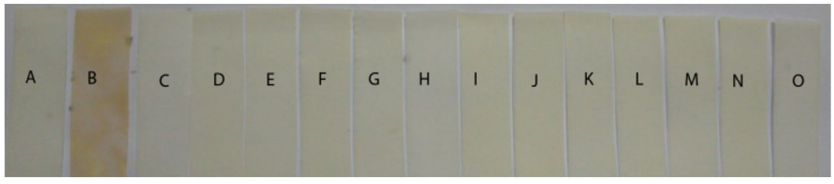

Figure 7. (Colour online) Colour change on paper strip of receptor **1** on treatment with one equivalent tetrabutylammonium salt of different anions in DMSO:water (8:2, 1.0 mM TRIS buffer, pH 7.6) [**1**] = 1.96×10^{-5} M. From left to right; A = Free receptor, B = CN^-, C = F^-, D = OAc^-, E = Cl^-, F = Br^-, G = I^-, H = NO_3^-, I = $H_2PO_4^-$, J = HSO_4^-, K = PF_6^-, L = PhO^-, M = ClO_4^-, N = S^{2-}, O = SH^-,= 1.96×10^{-5} M.

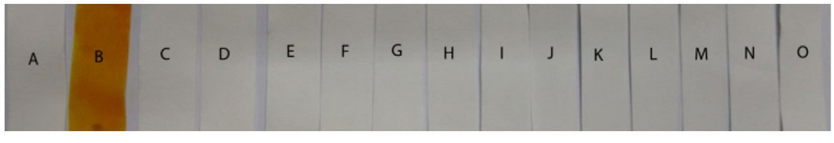

Figure 8. (Colour online) Colour change on paper strip of receptor **2** on treatment with one equivalent tetrabutylammonium salt of different anions in DMSO:water (8:2, 1.0 mM TRIS buffer, pH 7.6) [**2**] = 1.96×10^{-5} M. From left to right; A = Free receptor, B = CN^-, C = F^-, D = OAc^-, E = Cl^-, F = Br^-, G = I^-, H = $H_2PO_4^-$, I = HSO_4^-, J = PF_6^-, K = PhO^-, L = ClO_4^-, M = S^{2-}, N = SH^-, O = NO_3^- = 1.96×10^{-5} M.

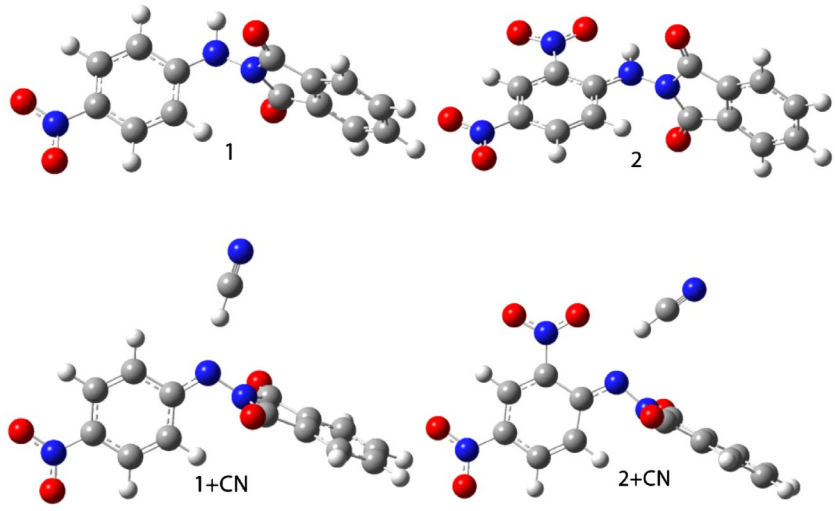

Figure 9. (Colour online) The B3LYP/6-31+G(d,p) optimised geometries of the free receptors **1**, **2** and their complex with the cyanide ion.

Table 4. The energy of the free receptors **1**, **2** and their complex with cyanide ion calculated using DFT/B3LYP/6-31+G(d,p) and MPW1PW91/6-31+G(d,p) methods.

Receptor	Energy (kcal/mol)		Total energy of free **1** or **2** + free CN^- Ions B3LYP (MPW1PW91)	$\Delta E = E_{complex} - E_{receptor} - E_{CN}$– B3LYP (MPW1PW91)
	B3LYP/6-31+G(d,p) (ΔE_{solv})	MPW1PW91/6-31+G(d,p) (ΔE_{solv})		
1	−630,031.58 (−13.99)	−629,880.40 (−13.70)		
1+CN	−688,342.24 (−46.59)	−688,169.21 (−46.72)	−688,305.52 (−688,131.39)	−36.72 (−37.82)
2	−758,361.19 (−14.32)	−758,178.80 (−13.63)		
2+CN	−816,674.66 (−46.46)	−816,470.24 (−46.47)	−816,635.12 (−816,429.79)	−39.54 (−40.44)

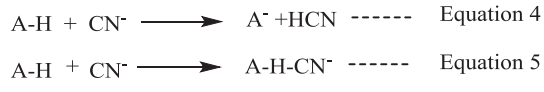

Scheme 3. Equations representing the complexation models.

was observed. For example, the N_3-N_6-C_9 angle in the receptor **1** calculated using B3LYP (120.10°) and MPW1PW91 (120.20°) methods were observed to correlate well with the angle observed in the same set of atoms (N_4-N_3-C_{10}) in the crystal structure (119.8(3)°). Similarly, The N-N-C angle in the receptor **2** calculated using B3LYP (N_5-N_9-C_{13}, 122.27°) and MPW1PW91 (N_5-N_9-C_{12}, 121.99°) methods were observed to correlate well with the angle observed for the same set of atoms (N_5-N_9-C_{12}) in the geometry obtained through the crystal structure (120.57(4)°).

The energy of the free receptor and cyanide ion was compared with the energy of the complex using equation 4 and 5 (Scheme 3).

Both equations indicated that both receptors **1** and **2** can form a stable complex with the cyanide ion. When equation 4 was used for ΔE calculation using MPW1PW91 ($\Delta E = E_{rec-H} + E_{CN}^- - E_{rec} - E_{HCN}$), the equation 4 yielded a value of −22.11 kcal/mol for receptor **1** and −25.39 kcal/mol for receptor **2**. When equation 5 was used for calculation of ΔE for the reaction, a value of −37.82 and −40.44 kcal/mol was observed, which indicated that the equation 5 provide the more stable geometry of the complex between receptor and cyanide ion. Therefore, the DFT methods supported the formation of a stable complex geometry, where HCN is linked to receptor **1** and **2** through hydrogen bond. It was concluded that cyanide ion first abstracts a proton from the receptor followed by formation of H-bond between negatively charged receptor and cyanide ion. The energy difference calculated by MPW1PW91 and B3LYP method differs only by 1 kcal/mol indicating that B3LYP method can be used for such studies. The solvation energy calculated using B3LYP and MPW1PW91 indicated that the cyanide complex is further stabilised by polar solvent like DMSO, which indicate the polar nature of the complex. The theoretical investigations also suggested that the receptor **2** should form a more stable complex with cyanide ion in comparison to the receptor **1**. The greater stability of the **2**-CN complex predicted by quantum chemical methods corroborates the experimental results. The ratio of binding constant value **2**-CN/**1**-CN (1.11) and the calculated ratio of $\Delta E_{2-CN}/\Delta E_{1-CN}$ (1.08_{B3LYP}, $1.07_{MPW1PW91}$) indicates a good correlation between the experimentally observed data and calculated data.

To investigate the observed UV–visible spectra of the receptor **1** and **2** on the addition of cyanide ions, calculations using TD-DFT/B3lYP/6-31+G(d,p) method were

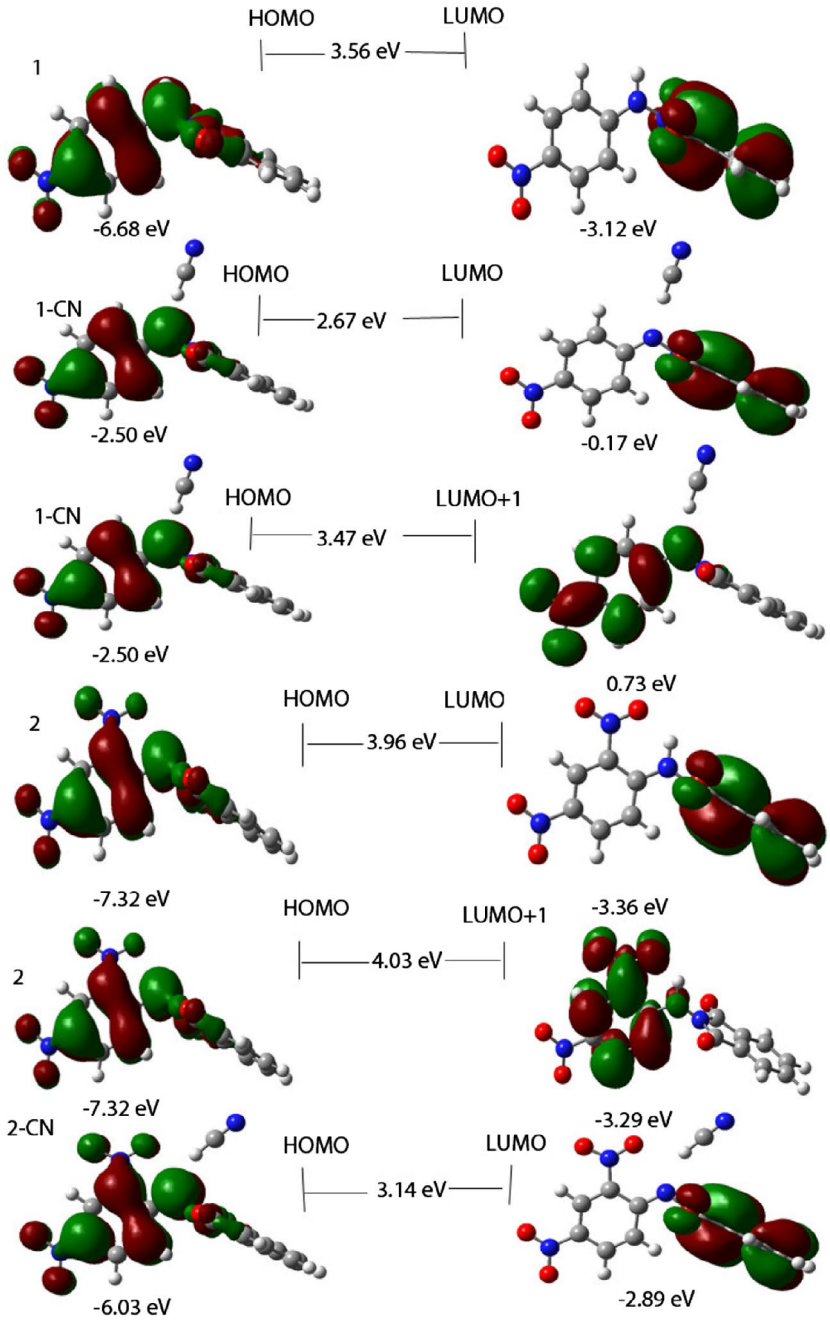

Figure 10. (Colour online) Energy diagrams depicting the main orbitals of receptors **1**, **2** and their **1**-CN, **2**-CN complex, calculated using the TD-DFT/B3LYP/6-31+G(d,p) method.

performed with Gaussian 09 software suite. The calculated electronic excitation parameters are listed in the Table S1 for receptors **1**, **2** and their **1**-CN and **2**-CN complex. The singlet electronic transition in receptor **1** was mainly contributed by HOMO to LUMO (S_0 to S_1) orbitals for the observed absorption band. The TD-DFT/B3LYP/6-31+G(d,p) calculated energy of HOMO to LUMO transition (2.86 eV, 433 nm) is close to the observed absorption band (420 nm, Figure 4) in receptor **1**. The singlet electronic excitations in the receptor **1**-CN complex were mainly contributed by HOMO to LUMO (S_0 to S_1) and HOMO to LUMO+1 (S_0 to S_2) orbitals (Figure 10, Table S1) which are responsible for the observed absorption band (Figure 4). The energy (2.68 eV, 463.12 nm) of HOMO to LUMO+1 is close to the absorption band observed in **1**-CN complex (~450 nm, Figure 4). For receptor **2**, the singlet electronic excitations were mainly contributed by HOMO to LUMO+1 (S_0 to S_1) and HOMO to LUMO (S_0 to S_2) orbitals (Figure 10, Table S1), which are responsible for the observed absorption bands (Figure 5). The calculated energy for HOMO to LUMO+1 and HOMO to LUMO transitions are close to the absorption bands in receptor **2**. The singlet electronic excitation in the receptor

2-CN is mainly contributed by HOMO to LUMO (S_0 to S_1) transition (Table S1, Figure 10). The energy of the HOMO to LUMO transition energy (2.73 eV, 452.64 nm) correlates well with the absorption band (centred around 450 nm, Figure 5) observed in the **2**-CN complex. When similar calculations were performed with MPW1PW91/6-31+G(d,p), no further improvement was observed. Similarly, when the TD-DFT calculations were performed on the optimised geometry of the negatively charged anion of receptor **1** and **2**, the results did not correlate with the experimental data.

4. Conclusions

We have synthesised two phthalimide–hydrazone receptors flanked by electron withdrawing nitro groups. The receptor **1** crystallised in the $p2_12_12_1$ space group, while the receptor **2** crystallised in the $Pna2_1$ space group from methanolic solution. The synthesised receptors **1** and **2** displayed selective colorimetric response towards cyanide ion. The receptor **1** with a single nitro group produced a colour change from colourless to yellow, while the receptor **2** with two electrons withdrawing nitro groups displayed a more intense red colouration in the presence of cyanide ion. The HypSpec program analysis indicated a strong binding affinity of the synthesised receptors towards cyanide ions. Job's plot and HypSpec program suggested the 1:1 complex stoichiometry between the synthesised receptors and cyanide ion. The DFT calculations further indicated that the receptor **2** forms a stronger complex with cyanide ion in comparison to the receptor **1**. The B3LYP and MPW1PW91 method provided almost similar results indicating that B3LYP method can be used to predict the complex formation in such systems. The solvation energy calculated using B3LYP (PCM model) or MPW1PW91 (PCM model) suggested that the polar solvent stabilises the complex which supports the formation of ions. Further, receptor **1** and **2** were used to develop a paper-based sensing strip for the detection of cyanide ions.

Acknowledgements

Authors are thankful to the Director, USIC University of Delhi for instrumental facilities. Authors are thankful to Mr. Mohd. Shoaib Ansari for recording the crystallographic data. The authors are also thankful to the Principal (Rev. Dr. V. Thampu), St. Stephen's College and Mr. K. M. Mathew (Bursar) for providing the necessary infrastructure.

Disclosure statement

No potential conflict of interest was reported by the authors.

Funding

This work was financially supported by UGC [number 41-235/2012]; DST Science and Engineering Research Board [number SB/FT/CS-054/2012].

References

(1) Duke, R.M.; McCabe, T.; Schmitt, W.; Gunnlaugsson, T. *J. Org. Chem.* **2012**, *77* (7), 3115–3126.
(2) Gunnlaugsson, T.; Glynn, M.; Tocci, G.M.; Kruger, P.E.; Pfeffer, F.M. *Coord. Chem. Rev.* **2006**, *250* (23–24), 3094–3117.
(3) Abraham, K.; Buhrke, T.; Lampen, A. *Arch. Toxicol.* **2015**, *90* (3), 1–16.
(4) Pearcy, K.; Elphick, J.; Burnett-Seidel, C. *Environ. Toxicol. Chem.* **2015**, *34* (7), 1642–1648.
(5) Suksai, C.; Tuntulani, T. *Chem. Soc. Rev.* **2003**, *32* (4), 192–202.
(6) Panda, M.; Robinson, N.C. *Biochemistry* **1995**, *34* (31), 10009–10018.
(7) Koenig, R. *Science* **2000**, *287* (5459), 1737–1738.
(8) Wang, F.; Wang, L.; Chen, X.; Yoon, J. *Chem. Soc. Rev.* **2014**, *43* (13), 4312–4324.
(9) Poulton, J.E. *Plant physiol.* **1990**, *94* (2), 401–405.
(10) Anzenbacher, P.; Tyson, D.S.; Jursíková, K.; Castellano, F.N. *J. Am. Chem. Soc.* **2002**, *124* (22), 6232–6233.
(11) Xu, Z.; Chen, X.; Kim, H.N.; Yoon, J. *Chem. Soc. Rev.* **2010**, *39* (1), 127–137.
(12) Lee, J.J.; Lee, S.Y.; Bok, K.H.; Kim, C. *J. Fluoresc.* **2015**, *25* (5), 1449–1459.
(13) Qu, W.; Gao, G.; Shi, B.; Zhang, P.; Wei, T.; Lin, Q.; Yao, H.; Zhang, Y. *Supramol. Chem.* **2014**, *26* (5–6), 403–408.
(14) Pati, P.B.; Zade, S.S. *Eur. J. Org. Chem.* **2012**, *2012* (33), 6555–6561.
(15) Hu, J.; Li, J.; Qi, J.; Sun, Y. *New J. Chem.* **2015**, *39* (5), 4041–4046.
(16) Sahoo, P.R.; Mishra, P.; Agarwal, P.; Gupta, N.; Kumar, S. *J. Incl. Phenom. Macrocycl. Chem.* **2016**, *84* (1–2), 163–171.
(17) Lv, X.; Liu, J.; Liu, Y.; Zhao, Y.; Chen, M.; Wang, P.; Guo, W. *Sens. Actuat. B* **2011**, *158* (1), 405–410.
(18) Batista, R.M.; Oliveira, E.; Costa, S.P.; Lodeiro, C.; Raposo, M.M.M. *Supramol. Chem.* **2014**, *26* (2), 71–80.
(19) Chow, C.-F.; Lam, M.H.W.; Wong, W.-Y. *Inorg. Chem.* **2004**, *43* (26), 8387–8393.
(20) Kim, Y.-H.; Hong, J.-I. *Chem. Commun.* **2002**, *5*, 512–513.
(21) Jin, W.J.; Fernández-Argüelles, M.T.; Costa-Fernández, J.M.; Pereiro, R.; Sanz-Medel, A. *Chem. Commun.* **2005**, *7*, 883–885.
(22) Touceda-Varela, A.; Stevenson, E.I.; Galve-Gasión, J.A.; Dryden, D.T.F.; Mareque-Rivas, J.C. *Chem. Commun.* **2008**, *17*, 1998–2000.
(23) Hudnall, T.W.; Gabbaï, F.P. *J. Am. Chem. Soc.* **2007**, *129* (39), 11978–11986.
(24) Badugu, R.; Lakowicz, J.R.; Geddes, C.D. *J. Am. Chem. Soc.* **2005**, *127* (10), 3635–3641.
(25) Shiraishi, Y.; Adachi, K.; Itoh, M.; Hirai, T. *Org. Lett.* **2009**, *11* (15), 3482–3485.
(26) Sahoo, P.; Prakash, K.; Kumar, S. *Supramol. Chem.* **2016**, 1–10doi:10.1080/10610278.10612016.11197398.
(27) Ajayakumar, M.R.; Mukhopadhyay, P.; Yadav, S.; Ghosh, S. *Org. Lett.* **2010**, *12* (11), 2646–2649.

(28) Ajayakumar, M.; Mukhopadhyay, P.; Yadav, S.; Ghosh, S. *Org. lett.* **2010**, *12* (11), 2646–2649.
(29) Ros-Lis, J.V.; Martínez-Máñez, R.; Soto, J. *Chem. Commun.* **2005**, *42*, 5260–5262.
(30) Hong, S.-J.; Yoo, J.; Kim, S.-H.; Kim, J.S.; Yoon, J.; Lee, C.-H. *Chem. Commun.* **2009**, *2*, 189–191.
(31) Sun, S.-S.; Lees, A.J. *Chem. Commun.* **2000**, *17*, 1687–1688.
(32) Amendola, V.; Esteban-Gómez, D.; Fabbrizzi, L.; Licchelli, M. *Acc. Chem. Res.* **2006**, *39* (5), 343–353.
(33) Bondy, C.R.; Gale, P.A.; Loeb, S.J. *J. Am. Chem. Soc.* **2004**, *126* (16), 5030–5031.
(34) Parthasarathi, R.; Subramanian, V.; Sathyamurthy, N. *J. Phys. Chem. A* **2006**, *110* (10), 3349–3351.
(35) Chudzinski, M.G.; McClary, C.A.; Taylor, M.S. *J. Am. Chem. Soc.* **2011**, *133* (27), 10559–10567.
(36) Subramanian, S.; Zaworotko, M.J. *Coord. Chem. Rev.* **1994**, *137*, 357–401.
(37) Choi, K.; Hamilton, A.D. *Coord. Chem. Rev.* **2003**, *240* (1–2), 101–110.
(38) Trzesowska, A. *J. Mol. Struct.* **2009**, *917* (2–3), 125–132.
(39) Upadhyay, K.; Mishra, R.K.; Kumar, A.; Zhao, J.; Prasad, R. *J. Mol. Struct.* **2010**, *963* (2–3), 228–233.
(40) Kok, S.H.L.; Gambari, R.; Chui, C.H.; Yuen, M.C.W.; Lin, E.; Wong, R.S.M.; Lau, F.Y.; Cheng, G.Y.M.; Lam, W.S.; Chan, S.H. *Bioorg. Med. Chem.* **2008**, *16* (7), 3626–3631.
(41) Santos, J.L.; Yamasaki, P.R.; Chin, C.M.; Takashi, C.H.; Pavan, F.R.; Leite, C.Q. *Bioorg. Med. Chem.* **2009**, *17* (11), 3795–3799.
(42) Singh, A.K.; Singh, R.K. *J. Mol. Struct.* **1089**, *2015*, 191–205.
(43) Su, X.; Aprahamian, I. *Chem. Soc. Rev.* **2014**, *43* (6), 1963–1981.
(44) Chen, G.; Wardle, N.J.; Sarris, J.; Chatterton, N.P.; Bligh, S.A. *Dalton Trans.* **2013**, *42* (39), 14115–14124.
(45) Sánchez-Sánchez, C.; Pérez-Inestrosa, E.; García-Segura, R.; Suau, R. *Tetrahedron* **2002**, *58* (36), 7267–7274.
(46) Pérez-Ruiz, R.; Díaz, Y.; Goldfuss, B.; Hertel, D.; Meerholz, K.; Griesbeck, A.G. *Org. Biomol. Chem.* **2009**, *7* (17), 3499–3504.
(47) Griesbeck, A.G.; Hanft, S.; Miara, Y.D. *Photochem. Photobiol. Sci.* **2010**, *9* (10), 1385–1390.
(48) Gottlieb, H.E.; Kotlyar, V.; Nudelman, A. *J. Org. Chem.* **1997**, *62* (21), 7512–7515.
(49) Frisch, M.J.; Trucks, G.W.; Schlegel, H.B.; Scuseria, G.E.; Robb, M.A.; Cheeseman, J.R.; Scalmani, G.; Barone, V.; Mennucci, B.; Petersson, G.A.; Nakatsuji, H.; Caricato, M.; Li, X.; Hratchian, H.P.; Izmaylov, A.F.; Bloino, J.; Zheng, G.; Sonnenberg, J.L.; Hada, M.; Ehara, M.; Toyota, K.; Fukuda, R.; Hasegawa, J.; Ishida, M.; Nakajima, T.; Honda, Y.; Kitao, O.; Nakai, H.; Vreven, T.; Montgomery, J.A., Jr.; Peralta, J.E.; Ogliaro, F.; Bearpark, M.; Heyd, J.J.; Brothers, E.; Kudin, K.N.; Staroverov, V.N.; Kobayashi, R.; Normand, J.; Raghavachari, K.; Rendell, A.; Burant, J.C.; Iyengar, S.S.; Tomasi, J.; Cossi, M.; Rega, N.; Millam, J.M.; Klene, M.; Knox, J.E.; Cross, J.B.; Bakken, V.; Adamo, C.; Jaramillo, J.; Gomperts, R.; Stratmann, R.E.; Yazyev, O.; Austin, A.J.; Cammi, R.; Pomelli, C.; Ochterski, J.W.; Martin, R.L.; Morokuma, K.; Zakrzewski, V.G.; Voth, G.A.; Salvador, P.; Dannenberg, J.J.; Dapprich, S.; Daniels, A.D.; Farkas, O.; Foresman, J.B.; Ortiz, J.V.; Cioslowski, J.; Fox, D.J. *Gaussian 09, Revision A.02*; Gaussian Inc, Wallingford, CT, 2009.
(50) Miertuš, S.; Scrocco, E.; Tomasi, J. *Chem. Phys.* **1981**, *55* (1), 117–129.
(51) Evans, T.W.; Dehn, W.M. *J. Am. Chem. Soc.* **1929**, *51* (12), 3651–3652.
(52) Parsons, S.; Flack, H.D.; Wagner, T. *Acta Cryst. B* **2013**, *69* (3), 249–259.
(53) Dolomanov, O.V.; Bourhis, L.J.; Gildea, R.J.; Howard, J.A.; Puschmann, H. *J. Appl. Cryst.* **2009**, *42* (2), 339–341.
(54) Sheldrick, G.M. *Acta Cryst. A* **2015**, *71* (1), 3–8.
(55) Sheldrick, G.M. *Acta Cryst. C* **2015**, *71* (1), 3–8.
(56) Macrae, C.F.; Bruno, I.J.; Chisholm, J.A.; Edgington, P.R.; McCabe, P.; Pidcock, E.; Rodriguez-Monge, L.; Taylor, R.; Streek, J.V.; Wood, P.A. *J. Appl. Cryst.* **2008**, *41* (2), 466–470.
(57) Zhu, X.; Lin, Q.; Lou, J.-C.; Lu, T.-T.; Zhang, Y.-M.; Wei, T.-B. *New J. Chem.* **2015**, *39* (9), 7206–7210.
(58) Kim, D.-S.; Chung, Y.-M.; Jun, M.; Ahn, K.H. *J. Org. Chem.* **2009**, *74* (13), 4849–4854.
(59) Sun, Y.; Wang, G.; Guo, W. *Tetrahedron* **2009**, *65* (17), 3480–3485.
(60) Park, J.; Kang, J. *J. Incl. Phenom. Macrocycl. Chem.* **2011**, *69* (1–2), 57–61.
(61) Choi, Y.; Kang, J. *J. Incl. Phenom. Macrocycl. Chem.* **2014**, *79* (1–2), 95–102.
(62) Taft, R.W.; Bordwell, F.G. *Acc. Chem. Res.* **1988**, *21* (12), 463–469.
(63) Zhang, C.; Liu, C.; Li, B.; Chen, J.; Zhang, H.; Hu, Z.; Yi, F. *New. J. Chem.* **2015**, *39*, 1968–1973.
(64) Gans, P.; Sabatini, A.; Vacca, A. *Talanta* **1996**, *43* (10), 1739–1753.
(65) Lee, H.J.; Park, S.J.; Sin, H.J.; Na, Y.J.; Kim, C. *New J. Chem.* **2015**, *39* (5), 3900–3907.
(66) Regulatory body: Enviornment Protection Agency, USA; Drinking water quality legislation of the United States, 1974; Safe Drinking Water Act PL 93-523, Subchapter 6A of Title 42.
(67) Ding, Y.; Li, T.; Zhu, W.; Xie, Y. *Org. Biomol. Chem.* **2012**, *10* (21), 4201–4207.
(68) Tomasulo, M.; Raymo, F.M. *Org. Lett.* **2005**, *7* (21), 4633–4636.
(69) Ren, J.; Zhu, W.; Tian, H. *Talanta* **2008**, *75* (3), 760–764.
(70) Shiraishi, Y.; Sumiya, S.; Hirai, T. *Chem. Commun.* **2011**, *47* (17), 4953–4955.
(71) Zhu, S.; Li, M.; Sheng, L.; Chen, P.; Zhang, Y.; Zhang, S.X.-A. *Analyst* **2012**, *137* (23), 5581–5585.
(72) Badugu, R.; Lakowicz, J.R.; Geddes, C.D. *Anal. Chim. Acta* **2004**, *522* (1), 9–17.
(73) Badugu, R.; Lakowicz, J.R.; Geddes, C.D. *Dyes Pigments*. **2005**, *64* (1), 49–55.
(74) Wang, Y.; Kim, S.-H. *Dyes Pigments* **2014**, *102*, 228–233.
(75) Kumar, S.; Velasco, K.; McCurdy, A. *J. Mol. Struct.* **2010**, *968* (1–3), 13–18.
(76) Lu, N.T.; Nguyen, V.N.; Kumar, S.; McCurdy, A. *J. Org. Chem.* **2005**, *70* (22), 9067–9070.
(77) Cohen, A.J.; Mori-Sánchez, P.; Yang, W. *Chem. Rev.* **2012**, *112* (1), 289–320.
(78) Areán, C.O.; Palomino, G.T.; Carayol, M.R.L.; Pulido, A.; Rubeš, M.; Bludský, O.; Nachtigall, P. *Chem. Phys. Lett.* **2009**, *477* (1–3), 139–143.
(79) Nashed, R.; Ismail, Y.; Allam, N.K. *J. Renew. Sustain. Ener.* **2013**, *5* (2), 022701.
(80) Park, H.; Millis, A.J.; Marianetti, C.A. *Phys. Rev. Lett.* **2012**, *109* (15), 156402.
(81) Tsuzuki, S.; Lüthi, H.P. *J. Chem. Phys.* **2001**, *114* (9), 3949–3957.
(82) Zhao, Y.; Truhlar, D.G. *J. Phys. Chem. A* **2004**, *108* (33), 6908–6918.

(83) Zhao, Y.; Truhlar, D.G. *J. Chem. Theory Comput.* **2005**, *1* (3), 415–432.
(84) Oh, D.-S.; Choe, J.-I. *Bull. Korean Chem. Soc.* **2007**, *28* (4), 596–600.
(85) Rozhenko, A.B.; Schoeller, W.W.; Letzel, M.C.; Decker, B.; Agena, C.; Mattay, J. *J. Mol. Str.* **2005**, *732* (1–3), 7–20.
(86) Zhao, Y.; Tishchenko, O.; Truhlar, D.G. *J. Phys. Chem. B* **2005**, *109* (41), 19046–19051.
(87) Lynch, B.J.; Fast, P.L.; Harris, M.; Truhlar, D.G. *J. Phys. Chem. A* **2000**, *104* (21), 4811–4815.